Hydrogen-induced phase separation in amorphous $Cu_{0.5}Ti_{0.5}$ alloys.
I. Room-temperature experiments

B. Rodmacq

Groupe Métallurgie Physique, Service de Physique, Département de Recherche Fondamentale,
Centre d'Etudes Nucléaires de Grenoble, 85 X-38041 Grenoble Cédex, France

M. Maret

Laboratoire de Thermodynamique et Physico-Chimie Métallurgiques, Boîte Postale 75, 38402 St. Martin d'Hères Cédex, France

J. Laugier

Groupe Structures, Service de Physique, Département de Recherche Fondamentale, Centre d'Etudes Nucléaires de Grenoble,
85 X-38041 Grenoble Cédex, France

L. Billard and A. Chamberod

Groupe Métallurgie Phyisique, Service de Physique, Département de Recherche Fondamentale, Centre d'Etudes Nucléaires de Grenoble,
85 X-38041 Grenoble Cédex, France

The influence of hydrogen on the structure of an amorphous $Cu_{0.5}Ti_{0.5}$ alloy has been studied by means of x-ray and neutron scattering. These experiments include large-angle x-ray and neutron scattering and small-angle neutron scattering with hydrogen-deuterium substitution. The results indicate that large hydrogen contents (hydrogen-to-metal ratio of 0.84) induce a phase separation into Cu and TiH_x regions on a scale of about 10–15 Å. Experiments on samples loaded with hydrogen by electrolysis or from the gas phase show that such a phase separation does not depend on the method of hydrogen loading. The results of a computer simulation with nearest-neighbor Cu-Ti permutations reproduce the main features of the diffraction data and confirm the large change of chemical ordering between Cu and Ti atoms upon hydrogen absorption.

I. INTRODUCTION

Numerous studies on amorphous copper-titanium hydrides have been published. The major reasons for such an interest are (i) the possibility of introducing larger quantities of hydrogen in the amorphous alloys than in the corresponding crystalline compounds,[1] thus leading to potential technological applications, and (ii) the use of the light hydrogen atom as a local probe for both a better understanding of the structure of these amorphous alloys and a determination of the location of hydrogen.[2,3] Concerning the hydrogen-absorption capacity, it is well established[1,4] that the maximum hydrogen content in these amorphous Cu-Ti hydrides is directly related to the alloy composition, i.e., it increases with increasing titanium concentration. In addition the hydrogen-to-titanium ratio also increases with the titanium concentration, indicating that not only the number but also the local environment of the titanium atoms (existence of tetrahedral Ti_4 sites) influences the hydrogen-absorption capacity.

Nevertheless, the large hydrogen-absorption capacity in amorphous Cu-Ti hydrides cannot be explained on the basis of previous neutron scattering results on nonhydrogenated Cu-Ti amorphous alloys[3,5] which showed the existence of chemical ordering with a preference for unlike neighbors, thus decreasing the number of possible tetrahedral-like Ti sites. This was confirmed by comput-er simulation experiments of the structure of $Cu_{0.5}Ti_{0.5}$ amorphous alloys[6] which showed that the introduction of chemical ordering between Cu and Ti atoms led to a good agreement between experimental and simulated pair-correlation functions. Nevertheless the analysis of the computer model showed that the resulting maximum hydrogen capacity (considering only Ti_4 sites) was 0.12 hydrogen atoms per metal atom, much smaller than the one experimentally obtained (no other sites such as Ti_3Cu were considered in the simulation since Cu-H correlations were not observed in the experimental pair-correlation functions).

Such a discrepancy can be removed if one supposes that hydrogen not only occupies interstitial sites in the structure of the starting alloy but also modifies this structure so as to create more energetically favorable sites. Under these circumstances hydrogen can no longer be considered as a probe in a quasirigid matrix (neglecting expansion effects) but as a constituent of a ternary Cu-Ti-H alloy. A supplementary problem has now to be solved; that is, the structure of the hydrogenated alloy, in addition to problems of the structure of the as-prepared alloy and of the location of hydrogen.

A complication of such studies comes from the poor thermal stability of Cu-Ti-H amorphous alloys.[7,8] Whereas amorphous $Cu_{0.5}Ti_{0.5}$ and crystalline $(Cu_{0.5}Ti_{0.5})H_{0.48}$ alloys have transformation temperatures

of 715 and 637 K, respectively (with a heating rate of 20 K/min), the amorphous hydride $(Cu_{0.5}Ti_{0.5})H_{0.7}$ transforms irreversibly into copper and titanium hydride at 509 K. As noted in Ref. 7 such a transformation requires long-range movement of metal atoms at a relatively low temperature, which again indicates that hydrogen is more than an interstitial atom in the amorphous structure. Such poor thermal stability does not facilitate studies on the hydrogen mobility in these alloys which have to be limited to a relatively small temperature range.[9]

Apart from the above-mentioned apparent contradiction between calculated[6] and experimental[1] maximum hydrogen-to-metal ratio in $Cu_{0.5}Ti_{0.5}$ glasses, there are other experimental results which indicate that hydrogen indeed modifies the structure of the matrix. First, the interference functions and pair-correlation functions obtained from x-ray experiments on $(Cu_xTi_{1-x})H_y$ glasses[2] are greatly modified as the hydrogen content increases. Taking into account both the small difference in the x-ray scattering factors of copper and titanium and the very small weight of the hydrogen contribution, such large modifications of the curves are difficult to explain in the case of a simple filling of interstitial sites. Second, neutron scattering experiments[3] have shown the existence of a maximum at low angle, which indicates a nonhomogeneous distribution of the hydrogen atoms. In the case of $Cu_{0.67}Ti_{0.33}$ glasses, the combination of neutron scattering with hydrogen-deuterium substitution and anomalous small-angle x-ray scattering on both copper and titanium edges[10,11] support the hypothesis of a hydrogen-induced small-scale phase separation between titanium hydride and copper.

The present paper is devoted to an extensive study of the structure of electrolytically charged $(Cu_{0.5}Ti_{0.5})H_{0.84}$ glasses. Paper I presents both x-ray and neutron diffraction results which confirm the existence of phase separation induced by the introduction of hydrogen. These findings are then used in a computer simulation of the structure of the CuTi matrix. Some results obtained on samples prepared by reaction with hydrogen gas are also presented and lead to the same conclusions. Paper II[12] will concentrate on the thermal evolution of these glassy hydrides for different hydrogen contents as studied by calorimetry and neutron diffraction. It will also correlate these results with those obtained previously from small-angle neutron scattering experiments.[13]

II. SAMPLE PREPARATION

Amorphous $Cu_{0.5}Ti_{0.5}$ alloys were obtained by the melt-spinning technique in the form of ribbons 8-mm wide and 40-μm thick. They were loaded with hydrogen or deuterium by electrolysis in a diluted $HClO_4$ solution in H_2O (D_2O) with a current density of 5 A m^{-2} for 20 h. Mixtures of H_2O and D_2O were also used for the partially deuterated samples.

The total (H,D) content of the samples was determined through the pressure variation in a closed vessel containing about 1 g of sample during heating up to 1100 K. Hydrogen (deuterium) contents of 84±2 at. % were thus measured, corresponding to the composition

$(Cu_{0.5}Ti_{0.5})(H,D)_{0.84}$ or $CuTi(H,D)_{1.68}$. In the case of hydrogenated samples these concentrations were checked by neutron scattering by taking advantage of the large incoherent scattering cross section of hydrogen [$\sigma_{inc} = 81.67 \times 10^{-24}$ cm^2 (Refs. 14 and 15)]. The incoherent intensities were compared to those obtained from known amounts of TiH_2 powder (diluted into Al_2O_3 powder in order to get similar transmission coefficients). Hydrogen contents determined in this way were found to agree with those obtained from desorption experiments within a few percent.

The hydrogen-to-deuterium ratio in the partly deuterated samples was determined as follows. After the samples were heated above the crystallization temperature,[12] neutron diffraction spectra were recorded, and the intensities of the diffraction peaks of the $Ti(H,D)_x$ phase were measured. From the relative intensities of the peaks it was possible to determine the mean neutron scattering length of the (H,D) atoms and thus the proportion of hydrogen and deuterium in the samples.

Neutron and x-ray diffraction experiments were also performed on sputtered samples loaded with hydrogen from the gas phase. The samples were prepared by dc sputtering under 50 Pa of argon onto a liquid-nitrogen-cooled copper substrate in the form of disks 70 mm in diameter and 30–40-μm thick. As the surface of these Cu-Ti glasses passivates very rapidly in air, the samples were hydrogenated *in situ* just after sputtering by evacuating the chamber to 10^{-2} Pa and introducing 10^5 Pa of pure hydrogen gas in the sputtering chamber. Under these conditions absorption of hydrogen takes place very rapidly (within a few minutes). The hydrogen content in these samples was found to be slightly smaller than the one obtained by electrolytic charging. This could be due to a progressive passivation of the surface since we observed that keeping the sample a few hours under a vacuum of 10^{-2} Pa prevented subsequent hydrogen absorption.

III. LARGE-ANGLE X-RAY DIFFRACTION

A. Experiment

X-ray experiments were performed on a Philips horizontal diffractometer with molybdenum $K\alpha$ radiation ($\lambda = 0.711$ Å) in a $\theta, 2\theta$ transmission geometry. Since hydrogen loading causes embrittlement of the Cu-Ti glasses, the hydrogenated samples were crushed into a fine powder, stuck onto Scotch tape and placed on an aluminum holder into the chamber, which was subsequently evacuated in order to eliminate parasitic air scattering.

A computer-driven Si(Li) solid detector was used for recording the scattered intensity at 400 points with a counting time of 6 min per point for scattering angles 2θ from 40 to 130° corresponding to a q range ($q = 4\pi \sin\theta/\lambda$) from 0.62 to 16.1 Å^{-1}. From the intensities diffracted by the sample holder (Scotch tape) $I_s(q)$ and by sample holder plus sample $I_0(q)$ we can determine the scattered intensity per atom $I_a(q)$ by neglecting the absorption of x-ray photons in the Scotch tape:

$$I_0(q) = K \times P(q)[\, A\,(\mu,q) \times I_a(q) + A_c(\mu,q) \times C(q)\,]$$

$$+ A_s(\mu,q) \times I_s(q) \,,$$

where K is the normalization constant, $P(q)$ the polarization factor, μ the linear absorption coefficient of the sample, $A\,(\mu,q)$ the absorption term for the coherent radiation, $A_c(\mu,q)$ the absorption term for the Compton radiation, $A_s(\mu,q)$ the corrective term for the absorption by the sample of the x-ray photons scattered coherently by the Scotch tape, and $C(q)$ the Compton scattering factors calculated from Cromer's tables.[16]

If μ is known, A, A_c, and A_s can be determined.[17] K is calculated using the Norman's relation.[18] From $I_a(q)$ one can calculate the interference function $I(q)$ as

$$\langle f \rangle^2 I(q) = I_a(q) + \langle f \rangle^2 - \langle f^2 \rangle \,,$$

with $\langle f \rangle = \sum_i c_i f_i$ and $\langle f^2 \rangle = \sum_i c_i f_i^2$, where the f_i are the atomic scattering factors calculated through an analytic expression.[19]

The interference function $I(q)$ must oscillate around unity at large q. If the value of μ is too large or too small, $I(q)$ will oscillate around values larger or smaller than unity, respectively. The best value of μ is thus adjusted graphically by computer so as to give the correct behavior of $I(q)$ at large q. This very sensitive method is analogous to that of Ergun et al.[20]

In order to reduce the statistical fluctuations at large angles, the reduced interference function $q[I(q)-1]$ is then smoothed by a method using both cubic spline functions and least-squares criteria.[21] Finally, this smoothed function is truncated at a node q_n (i.e., $q_n[I(q_n)-1]=0$), generally the highest identifiable one, and the corresponding reduced atomic pair-distribution function $G(r)$ is obtained by a Fourier transform of $I(q)$:

$$G(r) = 4\pi r[\rho(r) - \rho_0]$$

$$= 2/\pi \int_0^{q_n} q\,[I(q) - 1]\sin(qr)dq \,,$$

where $\rho(r)$ is the atomic distribution function and ρ_0 the average atomic density.

B. Results

Figures 1 and 2 present the interference functions $I(q)$ and reduced atomic pair-distribution functions $G(r)$ for $Cu_{0.5}Ti_{0.5}$ and $(Cu_{0.5}Ti_{0.5})H_{0.84}$ alloys. The interference function in Fig. 1(a) is typical of amorphous samples with a first maximum at 2.9 Å^{-1} and second split maximum at 5.0 and 5.7 Å^{-1}. The $G(r)$ curve in Fig. 2(a) has a first maximum at 2.65 Å corresponding to the average of the Cu-Cu, Cu-Ti, and Ti-Ti nearest-neighbor distances.

As already reported by Grzeta et al.,[2] the introduction of hydrogen causes large changes in the shape of the interference function in Fig. 1(b) (smaller height and larger width of the first peak, disappearance of the splitting of the second peak). One can also observe the appearance of a small-angle signal. The changes in real space are also quite important. The first peak in Fig. 2(b) is clearly split into two peaks, the largest one at 2.55 Å and the smallest at 3.05 Å. The oscillations are more rapidly damped at

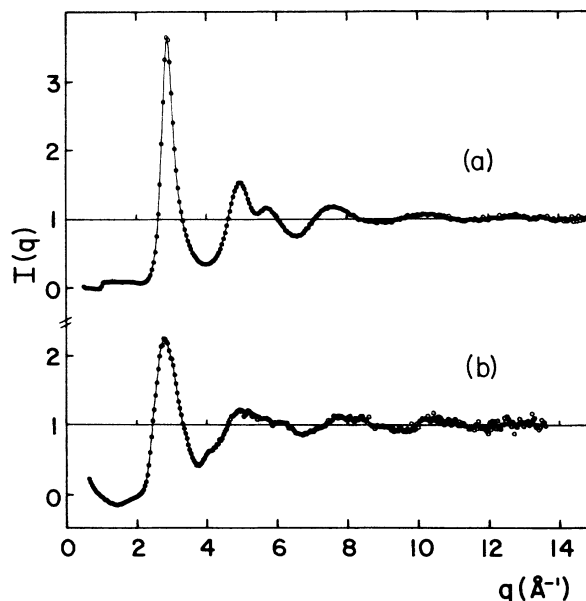FIG. 1. X-ray interference functions for (a) $Cu_{0.5}Ti_{0.5}$ and (b) $(Cu_{0.5}Ti_{0.5})H_{0.84}$ amorphous alloys.

larger distances and the splitting of the second peak is reversed compared to that of Fig. 2(a).

Such large changes in the $G(r)$ curves upon hydrogen absorption can have mainly two origins. In the formalism of Faber and Ziman[22] the total pair-correlation function can be decomposed into six partial functions $G_{ij}(r)$ (for a ternary alloy) according to

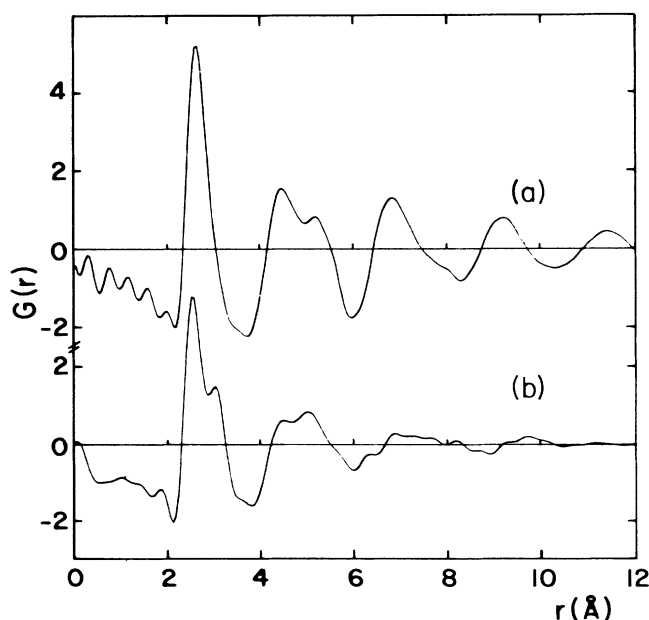$$G(r) = \sum_{i,j} W_{ij} G_{ij}(r), \quad i,j = \text{Cu, Ti, H}$$

FIG. 2. Reduced atomic distribution functions for (a) $Cu_{0.5}Ti_{0.5}$ and (b) $(Cu_{0.5}Ti_{0.5})H_{0.84}$ amorphous alloys.

TABLE I. Weights of the partial contributions to the total $G(r)$ for $(Cu_{0.5}Ti_{0.5})H_{0.84}$ alloys (x ray).

Cu-Cu	Cu-Ti	Ti-Ti	Cu-H	Ti-H	H-H
0.303	0.460	0.174	0.035	0.027	0.001

with

$$W_{ij} = \frac{c_i c_j f_i f_j}{\langle f \rangle^2}, \quad \text{and} \quad \langle f \rangle = \sum_i c_i f_i .$$

Table I gives the values of W_{ij} for the $(Cu_{0.5}Ti_{0.5})H_{0.84}$ alloys. One can see that the major contribution to the total $G(r)$ comes from the metal-metal correlations and that the Cu-Ti contribution dominates over the Cu-Cu and Ti-Ti ones. According to that, the filling of interstitial sites by the hydrogen atoms should only be detected in x-ray experiments through an increase of the metal-metal distances, owing to the small scattering factor of hydrogen.

The splitting of the first peak of $G(r)$ can first arise from an increase of the Ti-Ti nearest-neighbor distances, with little or no change of the corresponding Cu-Cu and Cu-Ti distances. Such an explanation was given to account for x-ray scattering results on glassy Zr_2PdH_3 hydrides[23] which indeed showed the appearance of such a splitting due to an increase of only the Zr-Zr distance, implying that all the hydrogen atoms occupied only Zr_4 sites. The same reasoning cannot hold in the case of Cu-Ti hydrides since, according to our results of computer simulation on $Cu_{0.5}Ti_{0.5}$ amorphous alloys,[6] there are not enough Ti_4 sites in the alloy to accommodate all the hydrogen atoms. As a consequence, they have to occupy also other sites such as Ti_3Cu for example. Therefore we should observe an increase of both the Cu-Ti and Ti-Ti nearest-neighbor distances, which should prevent the appearance of a splitting of the first peak.

The other explanation is that hydrogen modifies the amorphous structure. We suggest that a decrease of the number of Cu-Ti nearest-neighbor atoms to the benefit of Cu-Cu and Ti-Ti ones can also produce a splitting of the first peak. The neutron diffraction results presented in the next paragraphs will confirm the occurrence of such an atomic rearrangement.

IV. LARGE-ANGLE NEUTRON DIFFRACTION

A. Experimental and data analysis

The neutron diffraction measurements were performed on the D4B diffractometer at the Institut Laue Langevin (Grenoble) using a wavelength of 0.7 Å. The amorphous samples were maintained in a vanadium container of 0.1-mm thickness and 5-mm diam and placed at the center of the vacuum chamber of D4B. The diffracted intensities were measured by two ^3He detectors of 64 cells each, located at 1.50 and 0.75 m from the sample, the counting rate of detector 2 being thus about 4 times higher than that of detector 1. The 2θ scattering angles covered were $2\theta_{min} = 4.0°$, $2\theta_{max} = 64.7°$ with an angular step of 0.1° for detector 1 and $2\theta_{min} = 46.2°$, $2\theta_{max} = 134°$ with an angular step of 0.2° for detector 2, corresponding to q ranges $(q = 4\pi \sin\theta/\lambda)$ of 0.6–9.6 Å^{-1} and 7.04–16.52 Å^{-1}, respectively. For the partly deuterated sample the q range was extended down to 0.25 Å^{-1}.

For each detector the raw data were corrected first for the container scattering and the sample self-absorption using the expressions of the absorption factors developed by Paalman and Pings[24] and calculated from the values given in Table II.[14,15] For the samples loaded with hydrogen or deuterium, the scattering cross section of light atoms decreases with q due to inelastic effects. Therefore, in the calculation of the absorption factors we used a scattering cross section of H or D averaged over a 2θ range between 0 and 180° on the basis of an ideal-gas model by Copley[25] (noted $\bar{\sigma}_s$ in Table II). Then the counting level of the detector 2 was reduced to that of the detector 1 using the overlapping angular range.

For the as-prepared $Cu_{0.5}Ti_{0.5}$ alloys, the intensities were then corrected for the isotropic multiple scattering,[26] for the inelastic scattering,[27] and for the incoherent scattering. In order to determine the coherent scattering cross section per atom $I_a(q)$, the normalization of the

TABLE II. Coherent scattering lengths (b_{coh}), incoherent scattering cross sections (σ_{incoh}), bound scattering cross sections (σ_s^{bound}), scattering cross sections averaged over 2θ range between 0° and 180° $(\bar{\sigma}_s)$, and absorption cross sections for $\lambda = 0.7$ Å (σ_a).

	b_{coh} $(10^{-12}$ cm)	σ_{incoh} (b)	σ_s^{bound} (b)	$\bar{\sigma}_s$ (b)	σ_a (b)
Cu	0.7718	0.44	7.93		1.47
Ti	−0.3438	2.57	4.06		2.372
H	−0.374	79.9	81.67	28.75	0.13
D	0.6674	2.04	7.64	3.8	0

scattered intensity was realized at high q value (see for example, Ref. 28). The total interference function $S(q)$ was then related to $I_a(q)$ by

$$S(q) = I_a(q)/\langle b^2 \rangle ,$$

with $\langle b^2 \rangle = \sum_i c_i b_{i,coh}^2$. For the $(Cu_{0.5}Ti_{0.5})(H,D)_{0.84}$ alloys the scattered intensity $I(q)$ decreases strongly with q as shown in Fig. 3 for $(Cu_{0.5}Ti_{0.5})H_{0.57}D_{0.27}$. This is due to the self-inelastic scattering of light atoms. The intensity $I(q)$ for these ternary alloys, corrected for container scattering and self-absorption, can be written as follows:

$$I(q) = C_0 \left[\frac{d\sigma_{dis}(q)}{d\Omega} + \left(\sum_{Cu,Ti} c_i(b_{i,coh}^2 + b_{i,inc}^2) \right. \right.$$
$$\left. + \frac{d\sigma_{mul}}{d\Omega} + \frac{d\sigma_{inel}(q)}{d\Omega} \right)$$
$$\left. + C_{H,D} \frac{d\sigma_{H,D}(q)}{d\Omega} \right] , \tag{1}$$

where C_0 is the normalization constant and $d\sigma_{dis}(q)/d\Omega$ is the distinct scattering cross section which represents the interference effects between metal, hydrogen, and deuterium atoms and produces the oscillations of $I(q)$. The terms in large parentheses (coherent, incoherent, multiple, and inelastic terms) concern only the metal atoms and yield a quite q-independent intensity which can be calculated as mentioned above for the unloaded Cu-Ti alloys. The last term is the self-scattering of the light atoms. For the deuterium loaded samples, this term can be evaluated from the expression of $S(q,\omega)$ for an ideal gas, integrated over the energy transfer ω.[25] However, for hydrogenated samples with a high hydrogen content, such a procedure cannot reproduce the experimental decrease of the intensity with q because of the large contribution of multiple scattering.
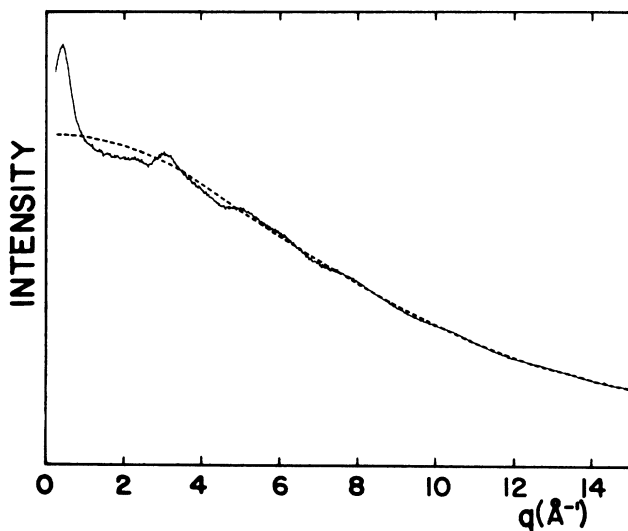

FIG. 3. Scattered intensity $I(q)$ of $(Cu_{0.5}Ti_{0.5})H_{0.57}D_{0.27}$ amorphous alloys. $I_s(q)$ (dashed line) passes through the oscillations of $I(q)$.

Therefore, in order to correct the experimental curves in the same manner for the hydrogenated and deuterated samples, we determined $d\sigma_{dis}(q)/d\Omega$ by calculating a smooth curve through the oscillations of $I(q)$. This curve is called $I_s(q)$ and represented by the dashed curve in Fig. 3. This function $I_s(q)$ is thus the sum of all the terms of Eq. (1), $d\sigma_{dis}(q)/d\Omega$ expected, and $I(q)$ can be written as

$$I(q) = C_0 \frac{d\sigma_{dis}(q)}{d\Omega} + I_s(q) .$$

Then, considering the first node q_0 of $d\sigma_{dis}(q)/d\Omega$, one can calculate the normalization constant C_0 from Eq. (1) and finally the total interference function $S(q)$ through

$$S(q) = 1 + \frac{d\sigma_{dis}(q)}{d\Omega} \bigg/ \langle b^2 \rangle$$

with

$$\frac{d\sigma_{dis}(q)}{d\Omega} = \frac{I(q) - I_s(q)}{C_0} .$$

The most serious drawback of such a normalization procedure is that it is rather difficult to estimate the value of $I_s(q)$ at small q. This leads to some uncertainty on the value of C_0 and thus on the amplitude of the oscillations of the resulting interference function. On the basis of the experimental results presented in this paper, a different way of determining $I_s(q)$ can be used and is presented in the Appendix. A rather good agreement is obtained when comparing the results of both methods, although the second procedure is physically more reasonable, at least in the system studied here.

B. Results

Figure 4 presents the interference functions $S(q)$ for $Cu_{0.5}Ti_{0.5}$ [Fig. 4(a)] and $(Cu_{0.5}Ti_{0.5})(H,D)_{0.84}$ alloys [Figs. 4(b)–4(d)]. The last three samples correspond to the compositions $(Cu_{0.50}Ti_{0.5})H_{0.57}D_{0.27}$, $(Cu_{0.5}Ti_{0.5})H_{0.84}$, and $(Cu_{0.5}Ti_{0.5})H_{0.08}D_{0.76}$. By comparison with the corresponding interference functions of Fig. 1 for x-ray scattering, one can notice an even larger change of the neutron $S(q)$ curves upon hydrogen or deuterium absorption. This is mainly due to the larger weights of the metal-hydrogen (deuterium) contributions compared to those in x-ray scattering. To illustrate this, Table III gives the weights of the different contributions for the four alloys studied. For the sake of comparison between the different curves, these weights are also given relative to that of the Cu-Cu contribution.

Although we said above that the modifications of the $S(q)$ curves are due to the large weight of the metal-hydrogen (deuterium) contributions, this is not the case for the curve of Fig. 4(b), where the mean scattering length of the (H,D) mixture is very small ($b_{H,D} = -0.039 \times 10^{-12}$ cm) as compared to those of hydrogen ($b_H = -0.374 \times 10^{-12}$ cm) or deuterium ($b_D = 0.6674 \times 10^{-12}$ cm). In this case, the total $S(q)$ is dominated by the metal-metal contributions, and thus

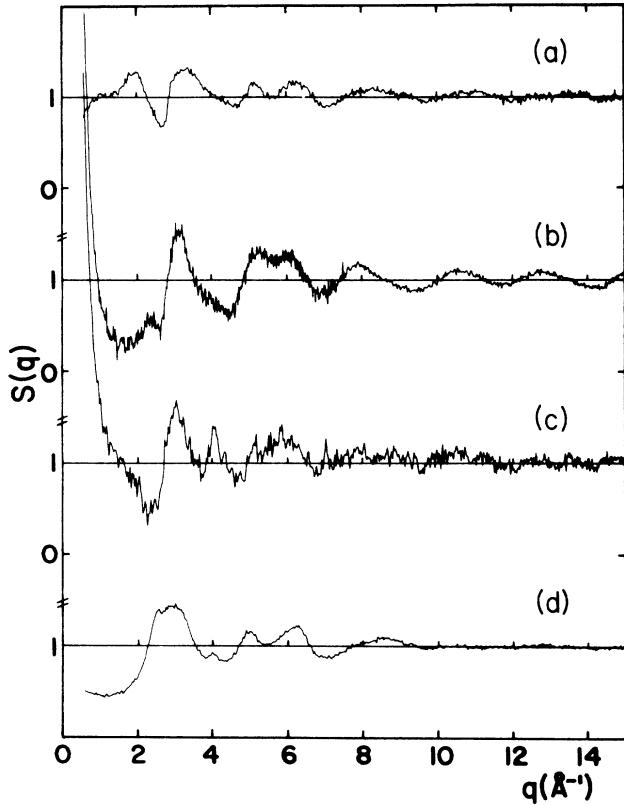FIG. 4. Neutron interference function $S(q)$ for (a) $Cu_{0.5}Ti_{0.5}$, (b) $(Cu_{0.5}Ti_{0.5})H_{0.57}D_{0.27}$, (c) $(Cu_{0.5}Ti_{0.5})H_{0.84}$, and (d) $(Cu_{0.5}Ti_{0.5})H_{0.08}D_{0.76}$ amorphous alloys.

FIG. 5. Reduced atomic distribution functions $G(r)$ for the same samples as in Fig. 4.

can be compared to that of the as-quenched sample in Fig. 4(a). As it was the case for the x-ray experiments, the important differences observed here between Figs. 4(a) and 4(b) thus mean that hydrogen loading leads to a large change of the structure of the metallic matrix. Such a change also results in the appearance of a strong small-angle signal in Figs. 4(b) and 4(c), but not in Fig. 4(d) for the deuterated sample. The origin of this small-angle signal will be given in the next section.

Figure 5 presents the reduced atomic distribution functions $G(r)$ obtained by a Fourier transform of the interference functions. Owing to the correction procedure in the case of hydrogenated and deuterated samples (cf.
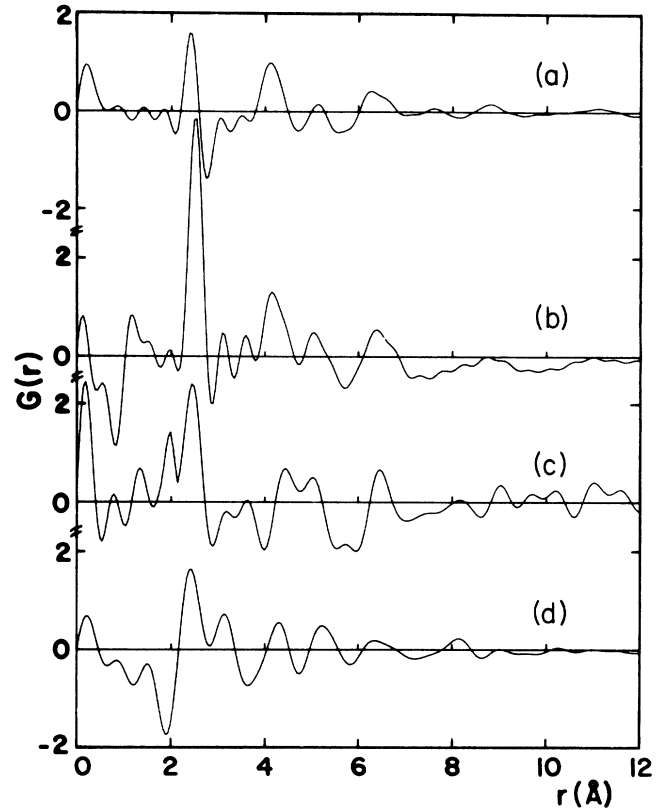
Sec. IV A), these curves exhibit some unphysical oscillations especially at small distances. Therefore we will restrict ourselves to a discussion about the variation of their main peaks with H or D loading.

The total $G(r)$ functions can be decomposed into six partial $G_{ij}(r)$ contributions ($i,j =$ Cu, Ti, H, or D) according to

$$G(r) = \sum_{i,j} W_{ij} G_{ij}(r) = \sum_{i,j} \frac{c_i c_j b_i b_j}{\langle b^2 \rangle} G_{ij}(r) .$$

The weights W_{ij} are given in Table III using an average coherent scattering length for the (H,D) mixture. As noted above, one can directly obtain information on the

TABLE III. Weights of the different contributions in $Cu_{0.5}Ti_{0.5}(H,D)_{0.84}$ alloys for neutron diffraction. Weights normalized to that of the Cu-Cu contribution are given in parentheses.

	$\bar{b}_{H,D}$ (10^{-12} cm)	Cu-Cu	Cu-Ti	Ti-Ti	Cu-H	Ti-H	H-H
$Cu_{0.5}Ti_{0.5}$		0.417	−0.372	0.083	0	0	0
		(1)	(−0.891)	(0.198)			
$(Cu_{0.5}Ti_{0.5})H_{0.57}D_{0.27}$	−0.039	0.226	−0.201	0.045	−0.039	0.017	0.002
		(1)	(−0.891)	(0.198)	(−0.171)	(0.076)	(0.007)
$(Cu_{0.5}Ti_{0.5})H_{0.84}$	−0.374	0.171	−0.152	0.034	−0.278	0.124	0.113
		(1)	(−0.891)	(0.198)	(−1.629)	(0.726)	(0.663)
$(Cu_{0.5}Ti_{0.5})H_{0.08}D_{0.76}$	+0.568	0.129	−0.115	0.026	0.319	−0.142	0.197
		(1)	(−0.891)	(0.198)	(2.475)	(−1.102)	(1.531)

hydrogen-induced modifications of the metallic matrix by comparing Figs. 5(a) and 5(b) since the weights of the metal-hydrogen (-deuterium) and hydrogen-hydrogen correlations are quite small for the sample of Fig. 5(b). Whereas the first positive $(r \simeq 2.4$ Å$)$ and negative $(r \simeq 2.75$ Å$)$ peaks in Fig. 5(a) can be attributed to Cu-Cu and Cu-Ti nearest-neighbor distances, respectively, it appears in Fig. 5(b) that the (H,D) loading leads principally to a large change of the relative intensities of these peaks. Such a modification can be assigned to a decrease of the number of Cu-Ti nearest-neighbor atoms to the benefit of the Cu-Cu ones upon hydrogen absorption. This result is in agreement with the splitting observed in x-ray experiments [Figs. 1(b) and 2(b)].

Concerning Figs. 5(c) and 5(d), hydrogen or deuterium loading leads to the appearance of a supplementary peak at about 1.9 Å. This peak is positive with hydrogen [Fig. 5(c)] and negative with deuterium [Fig. 5(d)]. According to Table III, this peak thus corresponds to titanium-hydrogen (-deuterium) correlations. Despite the much larger weight of the Cu-H (Cu-D) correlations as compared to the Ti-H (Ti-D) ones, there is no clear evidence of another negative (with H) or positive (with D) supplementary peak at about 1.5 Å (which would correspond to copper-hydrogen nearest-neighbor distances).

To summarize, it appears from both x-ray and neutron results that hydrogen loading of Cu-Ti glasses leads to a strong decrease of the Cu-Ti interactions and to the appearance of only Ti-H interactions. This unambiguously

shows that phase separation takes place upon hydrogen absorption. To illustrate this point, let us suppose that such a phase separation occurs between Cu and TiH_x microcrystals (these phases appear during the crystallization of the sample, see Paper II). It is thus possible to simulate the reduced atomic distribution functions of such a system starting from the stable fcc Cu and fcc TiH_x (with $x = 1.68$) phases and considering a Gaussian broadening of the peaks of the Patterson function in order to account for the small size of the crystals. Figure 6 shows the resulting $G(r)$ curves in the case of neutron scattering obtained by summing up both Cu and TiH_x, TiD_x, or $Ti(H,D)_x$ contributions according to their respective weights. These curves were obtained with lattice parameters $a_{Cu} = 3.55$ Å and $a_{TiH_x} = 4.35$ Å, both values slightly smaller than the bulk ones (3.61 and 4.45 Å, respectively). As compared to the corresponding experimental curves [Figs. 5(b)–5(d)], there is a qualitative agreement for both positions and relative intensities of the first peaks of $G(r)$, i.e., for the first metal-metal and metal-hydrogen distances.

As we will see in the following section, the phase separation is on a small scale; therefore a simple broadening of the peaks of the equilibrium phases is certainly not sufficient to account for the details of the experimental curves, because such a simplified model completely ignores possible Cu-Ti interactions. We will present in Sec. VI another way of simulating such a phase separation, starting from a model we already used in the case of nonhydrogenated Cu-Ti amorphous alloys.[6]

V. LOW-ANGLE NEUTRON DIFFRACTION

The samples used for these low-angle neutron diffraction studies were hydrogenated and deuterated under the same conditions as described in Sec. II. The experiments where carried out on the D1B diffractometer at the Institut Laue Langevin (Grenoble) using a wavelength of 2.52 Å. For the three alloys studied ($(Cu_{0.5}Ti_{0.5})H_{0.84}$, $(Cu_{0.5}Ti_{0.5})H_{0.69}D_{0.15}$, and $(Cu_{0.5}Ti_{0.5})D_{0.84}$, we observe in Fig. 7 a maximum at low angle, the high-q side corresponding to the strong small-angle increase in Figs. 4(b) and 4(c) [see also Fig. 9(b)]. The position of this maximum ($q = 0.4$ Å^{-1}) does not change with the hydrogen-deuterium substitution, but its intensity (measured above the incoherent background) decreases as the deuterium content increases. Such a behavior can be well explained by supposing that this maximum is an interference maximum in a two-phase system. In this case the small-angle intensity will be proportional to $\Phi(1-\Phi)(\rho_1-\rho_2)^2$ where Φ is the volume fraction of one phase and $\rho_1-\rho_2$ is the mean scattering length contrast between both phases. The variation of the intensity of the maximum with the (H,D) substitution implies that hydrogen (deuterium) is not uniformly distributed among both phases. More precisely, if one supposes that all the hydrogen belongs to only one of these phases, one can write

$$I \sim \Phi(1-\Phi)(\alpha_1 \bar{b}_H + \alpha_2)^2 \ ,$$

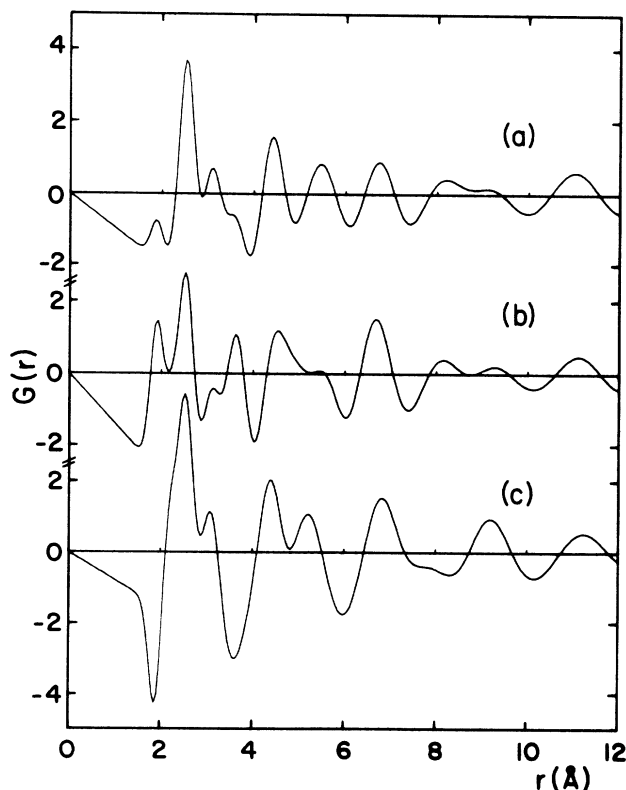where $\bar{b}_H$ is the mean scattering length of the (H,D) mix-

FIG. 6. Simulated atomic pair-distribution functions for (a) $(Cu_{0.5}Ti_{0.5})H_{0.57}D_{0.27}$ (b) $(Cu_{0.5}Ti_{0.5})H_{0.84}$, and (c) $(Cu_{0.5}Ti_{0.5})H_{0.08}D_{0.76}$ alloys.
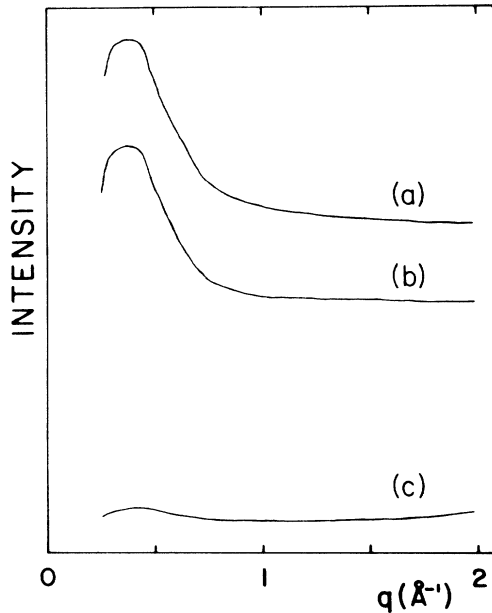
FIG. 7. Low-angle intensity vs scattering vector for (a) $(Cu_{0.5}Ti_{0.5})H_{0.84}$, (b) $(Cu_{0.5}Ti_{0.5})H_{0.69}D_{0.15}$, and (c) $(Cu_{0.5}Ti_{0.5})D_{0.84}$ alloys. The intensities are scaled to the same weight of sample.

ture and α_1 and α_2 are constants. Figure 8 presents a plot of $(I)^{1/2}$ as a function of $\bar{b}_H$, which shows that a straight line is indeed obtained. The intensity falls to zero for $\bar{b}_H = 1.04 \times 10^{-12}$ cm, at which value both phases have the same mean scattering length.

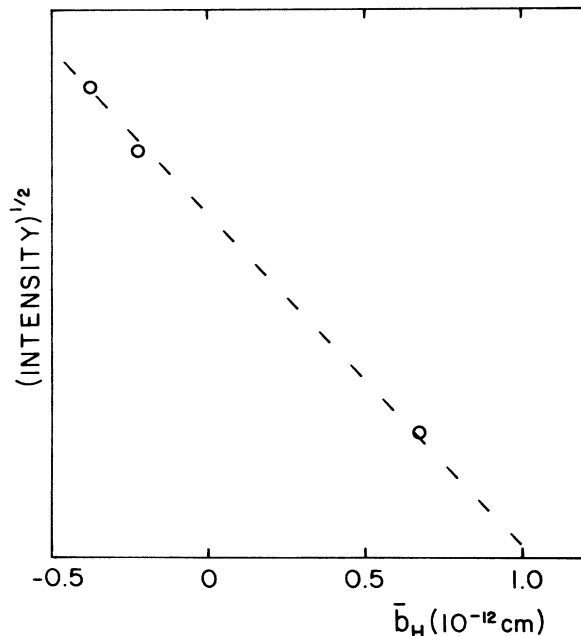Turning now to the chemical composition of the

FIG. 8. Square root of the intensity of the low-angle maximum as a function of the mean scattering length of the (H,D) mixture.

phases [i.e., the values of x and y if one supposes that the phases have the compositions $Cu_x Ti_y(H,D)_{0.84}$ and $Cu_{0.5-x}Ti_{0.5-y}$], a rough calculation of the variation of $\Delta\rho = \rho_1 - \rho_2$ as a function of x and y shows that $\Delta\rho$ is indeed equal to zero for y is equal to 0.5 (such a calculation is not very accurate because of the uncertainties on the densities of the phases). This calculation is less sensitive to the value of x; nevertheless x has to be small to account for the intensity of the maximum, as this intensity depends on the volume fraction of the phases. The phase separation is thus essentially between copper-rich and titanium hydride-rich regions.

Similar conclusions could be drawn from anomalous small-angle x-ray scattering measurements. In this case one takes advantage of the variation of the x-ray scattering factors of the metallic elements near the absorption edge.[29] Experiments carried out on the same samples used for the neutron study have shown that the variation of the intensity of the maximum at 0.4 Å^{-1} on both copper and titanium edges could be also explained by the presence of copper and titanium hydride regions,[30] as already observed in $(Cu_{0.67}Ti_{0.33})H_{0.34}$ alloys using the same technique.[10,11] One can note that both techniques are complementary, since the contrast variation concerns the metal atoms in the case of x-ray and the hydrogen atoms in the case of neutron scattering.

A last point concerns the extent of phase separation in these Cu-Ti alloys. From the position of the maximum, the mean correlation length of these phases can be estimated to about 10–15 Å ($\simeq 2\pi/q$). On such a small scale, any microcrystalline model (such as the one we presented in Sec. IV B) should take into account metal-metal correlations at the interfaces.

VI. NUMERICAL SIMULATION OF THE PHASE SEPARATION

We present here preliminary results of a computer simulation study of the structure of amorphous $Cu_{0.5}Ti_{0.5}$ hydrides. Our starting point is a model previously presented of the structure of nonhydrogenated Cu-Ti amorphous alloys.[6] We recalled in the Introduction that in this case we were unable to accommodate as much hydrogen as experimentally observed, because of the relatively small number of available Ti_4 tetrahedral sites. (This number was even smaller than that obtained with a random distribution of Cu and Ti atoms as a consequence of the observed chemical ordering in these glasses.[5]) Consequently we must now consider the change in the chemical ordering in Cu-Ti alloys (induced by the great affinity of hydrogen for titanium) as shown experimentally by the strong decrease of the Cu-Ti interactions [Fig. 5(b)] and the appearance of a small-angle maximum in $S(q)$ (Fig. 7).

From the initial $Cu_{0.5}Ti_{0.5}$ model of 1549 atoms[6] a Monte Carlo procedure is used to exchange Cu and Ti nearest-neighbor atoms (the first metal-metal distances are taken up to the first minimum after the first peak of each partial pair-correlation function, i.e., 3.08, 3.34, and 3.80 Å for Cu-Cu, Cu-Ti, and Ti-Ti pairs, respectively). Such an exchange is effectively realized if it leads to

an increase of the number of Ti-Ti pairs. This is equivalent to the Ising model with short-range interactions at zero temperature,[31] the only difference being that such a simulation is carried out here on an amorphous sample and not on the usual cubic lattice. When all possible permutations have been performed, the system is numerically relaxed using the same set of Johnson pair potentials as used for the as-prepared $Cu_{0.5}Ti_{0.5}$ glass. Then, from the positions of Cu and Ti atoms, we calculate the total pair-correlation function and then the total interference function. Partial coordination numbers can also be measured, from which one calculates the short-range order parameter.[32] Because of their size difference, Cu and Ti atoms tend to overlap upon permutation when a large atom replaces a small one, whereas free volumes are created in other regions when a small atom replaces a large one. Such a situation could be avoided to some extent by carrying out a numerical relaxation after every permutation. We did not use such a procedure here, because of the large computer time required (1600 permutations are necessary to reach the final state).

Figure 9 shows the simulated neutron interference function $S(q)$ and the experimental curve for the $(Cu_{0.5}Ti_{0.5})H_{0.57}D_{0.27}$ amorphous alloy. Since the contributions of the metal-hydrogen and hydrogen-hydrogen pairs are very small in this alloy (see Table III), a direct
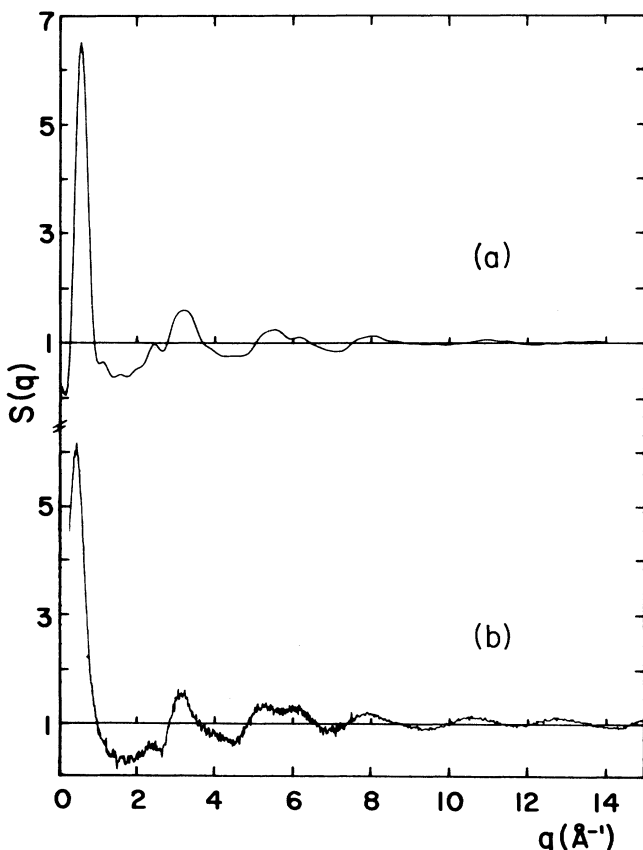
comparison of both curves is justified. As for Monte Carlo simulations of first-order transitions on cubic lattices,[31] the simulated $S(q)$ develops a well-defined small-angle maximum as observed experimentally. At larger q values the agreement is also satisfying. A small discrepancy in the period of the oscillations is however noticeable, probably because of the positions of the minimum of each metal-metal potential taken here identical to those used for the as-prepared glass. In real space both $G(r)$ curves are also very similar (curves not shown). They evidence the decrease of the number of unlike nearest-neighbor atoms. The short-range order parameter obtained from this model is $\alpha = +0.33$ compared to $\alpha = -0.08$ for the starting configuration.

It thus appears that the experimentally observed small-scale phase separation is well reproduced by our model. In addition, these calculations indicate that despite this rather large change of chemical order between copper and titanium the amorphous structure is still preserved. We plan to analyze the hydrogenation sites in order to get further comparison with experiments (maximum hydrogen capacity and metal-hydrogen correlations for example).

VII. SOME RESULTS ON PRESSURE-CHARGED SPUTTERED SAMPLES

It is interesting to know whether or not the phase separation observed in electrolytically charged samples is also present in samples loaded in hydrogen from the gas phase. To answer this question, sputtered $Cu_{0.5}Ti_{0.5}$ samples charged with hydrogen under pressure (see Sec. II) were studied by both x-ray and neutron scattering. We first checked that the x-ray and neutron interference functions for the as-sputtered sample were identical to those of the melt-spun one (except for a small hydrogen contamination of the sputtered sample only detectable through the slightly nonhorizontal background in neutron experiments). X-ray and neutron experiments were then performed after hydrogen loading and Fig. 10 presents the atomic distribution function for neutron diffraction to be compared to the corresponding one in Fig. 5(c).

In the case of x-ray experiments (curve not shown) the $G(r)$ curve is the same whatever the mode of charging, the only difference being that the splitting of the first peak (due to the small number of Cu-Ti nearest neighbors) is less well marked for the pressure-charged sample. In the case of neutron experiments, similar features are observed at small distances in Figs. 10 and 5(c), i.e., the appearance of Ti-H correlations at about 1.9 Å and the smaller amplitude of the first minimum after the Cu-Cu peak corresponding to the Cu-Ti correlations. We cannot comment on the differences at larger distances, because of the rather complicated normalization procedure of the diffraction curves in the case of hydrogenated samples (cf. Sec. IV).

In addition, low-angle x-ray and neutron experiments also show the presence of a small-angle maximum at about 0.5 Å^{-1}, thus indicating that the same tendency towards phase separation exists in these alloys. Finally, the

FIG. 9. Simulated neutron interference function for (a) $Cu_{0.5}Ti_{0.5}$ and experimental curve for (b) $(Cu_{0.5}Ti_{0.5})H_{0.57}D_{0.27}$ amorphous alloy.
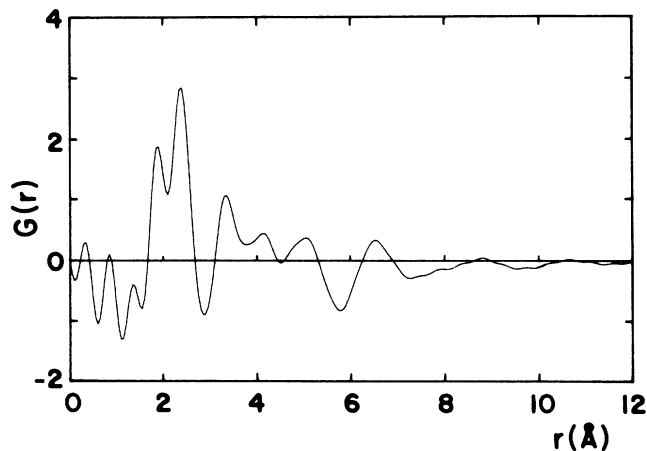
FIG. 10. Neutron atomic pair-distribution functions for $Cu_{0.5}Ti_{0.5}$ amorphous hydrides loaded from the gas phase.

similar behavior observed in calorimetry experiments (see Paper II) confirms that gas-charged samples are essentially identical to the electrolytically-charged ones.

VIII. CONCLUSION

To summarize, this extensive study of amorphous Cu-Ti hydrides shows that hydrogen absorption in these metallic glasses leads to a phase separation between copper-rich and titanium-hydrogen-rich regions. All the experimental results presented here (small-angle and large-angle x-ray and neutron scattering) indicate the formation of small ($\sim 10-15$ Å) Cu and TiH_x regions whatever the method of hydrogen loading (by electrolysis or from the gas phase). It also appears that such a phase separation does not depend on the alloy composition, as shown by previous anomalous x-ray and neutron scattering experiments on $Cu_{0.67}Ti_{0.33}$ hydrides.[11]

This study also explains the discrepancies we found, previously concerning the maximum hydrogen content of these alloys.[3,6] It is clear that if hydrogen loading leads to a reorganization of the metallic matrix so as to create more Ti-Ti interactions, the hypothesis of a "rigid matrix" used in our first computer simulations is no longer valid. Furthermore this could simply explain why the amorphous Cu-Ti hydrides absorb more hydrogen than the crystalline ones, because of the larger number of tetrahedral Ti_4 sites.

The existence of small TiH_x regions agrees quite well with our quasielastic neutron scattering results[33] which showed that hydrogen performs a fast localized motion and that more and more hydrogen atoms are trapped as their concentration increases.

Concerning the mechanism of formation of this small-scale phase separation, the thermal evolution (Paper II) indicates that such a structure does not change up to about 360 K at which temperature long-range crystallization takes place. This implies that a metastable configuration is achieved at room temperature. A possible explanation could be that hydrogen induces only

nearest-neighbor structural rearrangements between metal atoms (local Cu-Ti permutations for example) but no longer range reorganization. The result of such local permutations can be very well understood in the simple case of a unidimensional chain of (A,B) atoms. Starting for example from a chemically-ordered configuration with only A-B nearest-neighbor pairs, the permutations of these pairs will lead (i) to a decrease of the number of A-B pairs to the benefit of A-A and B-B ones, and (ii) to the appearance of a A-A-B-B ... super periodicity, which is directly related to the small-angle maximum in the scattering curve. This agrees with the preliminary simulation results presented here which show that such nearest-neighbor interchanges are sufficient to reproduce the main features of the diffraction curves.

Note added : Since this paper was submitted, Harris *et al.*[34] proposed a model for hydrogen absorption in amorphous transition-metal alloys on the basis of experimental results obtained in Ni-Zr-H glasses. Their claim that this model also applies to Cu-Ti-H glasses (i.e., hydrogen occupies Ti_4, Ti_3Cu, and a fraction of Ti_2Cu_2 tetrahedral sites of the chemically disordered Cu-Ti matrix) is clearly ruled out by the results presented here (no evidence of Cu-H correlations and segregation of Cu and Ti atoms upon absorption of hydrogen). We hope to comment further on their paper in a forthcoming publication which will present our results of computer simulation in more details.

ACKNOWLEDGMENTS
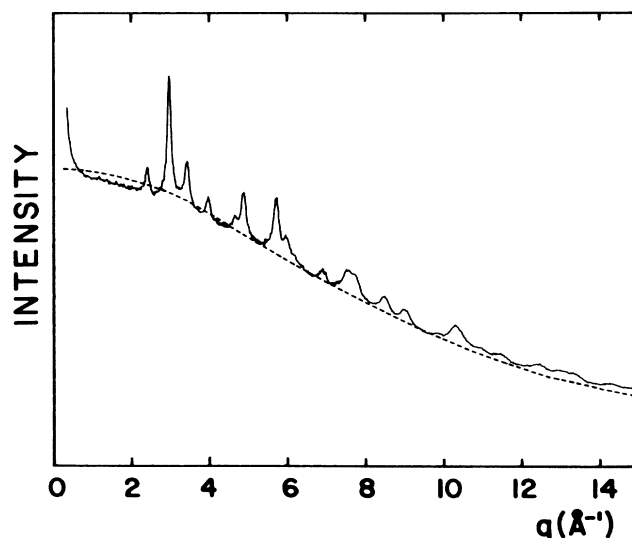
FIG. 11. Comparison between $I_s(q)$ of Fig. 3 and the scattering curve of a crystallized $(Cu_{0.5}Ti_{0.5})H_{0.57}D_{0.27}$ alloy.

APPENDIX

As noted in Sec. VI A, the main problem for the correction of the neutron scattering curves of hydrogenated amorphous samples is the strongly decreasing background due to the inelastic scattering of light atoms with a mass comparable to that of the incident neutron. To find an analytic expression for the q dependence of this contribution, one has to consider the interaction between the hydrogen atoms and the surrounding metal atoms. Expressions derived from models (ideal gas model[25]) or real systems (scattering from a water molecule[35]) can only be used for relatively small hydrogen contents, which is not the case for our Cu-Ti hydrides ($H/M = 0.84$).

Nevertheless another approach can be used in some cases by considering the scattering behavior of related crystalline hydrides. This supposes that the local environment of the hydrogen atoms in the amorphous alloy is not too different from that in the crystalline hydride. Such an approximation has been used for example by Chieux et al.[36] in amorphous Tb-Cu alloys with 4 at. % hydrogen by comparing the scattering curve of the amor-

phous alloy to that of a crystalline $TbH_{1.6}$ alloy.

Owing to the experimental results presented in this paper, it is tempting to use such an approach for Cu-Ti-H glasses since the local hydrogen environment appears to be similar to that found in crystalline titanium hydride. We thus performed neutron scattering experiments on our Cu-Ti-H alloys after heating above the transformation temperature. Since the corresponding diffraction curve now consists of Bragg peaks of Cu and TiH_x superimposed on the q-dependent background, it is thus easy to separate these two contributions. Figure 11 presents the diffraction curve of $(Cu_{0.5}Ti_{0.5})H_{0.57}D_{0.27}$ alloy after heating to 473 K along with the smooth curve determined in Sec. IV A and noted $I_s(q)$. The fact that $I_s(q)$ closely reproduces the q-dependent background of the crystallized sample justifies the procedure used in this paper. The advantage of the method proposed in this Appendix is that the shape of the curve at small q can be determined with more accuracy. But one should emphasize that this method is only valid in case where one has some evidence of similar local structure between the amorphous hydride and the crystalline hydride considered.

[1]A. J. Maeland, L. E. Tanner, and G. G. Libowitz, J. Less-Common Met. **74**, 279 (1980).

[2]B. Grzeta, K. Dini, N. Cowlam, and H. A. Davies, J. Phys. F **15**, 2069 (1985).

[3]B. Rodmacq, Ph. Mangin, and A. Chamberod, J. Phys. F **15**, 2259 (1985); B. Rodmacq, Ph. Mangin, L. Billard, and A. Chamberod, in *Hydrogen in Disordered and Amorphous Solids*, Vol. 136 of *NATO Advanced Study Institute, Series B: Physics*, edited by G. Bambakidis and R. C. Bowman (Plenum, New York, 1986), p. 303.

[4]A. J. Maeland, in *Metal Hydrides*, edited by G. Bambakidis (Plenum, New York, 1981), p. 177.

[5]M. Sakata, N. Cowlam, and H. A. Davies, in *Proceedings of the 4th International Conference on Rapidly Quenched Metals, Sendai, 1981*, edited by T. Masumoto and K. Suzuki (Japan Institute of Metals, Sendai, 1982), Vol. 1, p. 327.

[6]B. Rodmacq, L. Billard, Ph. Mangin, and A. Chamberod, J. Phys. (Paris) Colloq. **46**, C8-415 (1985).

[7]R. C. Bowman, Jr., R. J. Furlan, J. S. Cantrell, and A. J. Maeland, J. Appl. Phys. **56**, 3362 (1984).

[8]R. J. Furlan, G. Bambakidis, J. S. Cantrell, R. C. Bowman, Jr., and A. J. Maeland, J. Less-Common Met. **116**, 375 (1986).

[9]R. C. Bowman, Jr., A. J. Maeland, and W. K. Rhim, Phys. Rev. B **26**, 6362 (1982).

[10]Ph. Goudeau, A. Naudon, B. Rodmacq, Ph. Mangin, and A. Chamberod, J. Phys. (Paris) Colloq. **46**, C8-479 (1985).

[11]Ph. Goudeau, A. Naudon, A. Chamberod, B. Rodmacq and C. E. Williams, Europhys. Lett. **3**, 269 (1987).

[12]B. Rodmacq and A. Chamberod, following paper, Phys. Rev. B **38**, 1116 (1988).

[13]Ph. Mangin, B. Rodmacq, and A. Chamberod, Phys. Rev. Lett. **55**, 2899 (1985).

[14]L. Koester and W. B. Yelon, in *Neutron Diffraction Newsletter*, edited by W. B. Yelon (Neutron Diffraction Commission of the International Union of Crystallography, Columbia, 1983).

[15]V. F. Sears, Atomic Energy of Canada Limited, Report No. AECL-8490, Chalk-River, 1984 (unpublished).

[16]D. T. Cromer and J. B. Mann, J. Chem. Phys. **47**, 1892 (1967).

[17]F. Hajdu and G. Palinkas, J. Appl. Crystallogr. **5**, 395 (1972).

[18]N. Norman, Acta Crystallogr. **10**, 370 (1957).

[19]*International Tables of X-Ray Crystallography*, edited by J. A. Ibers and W. C. Hamilton (Kynoch, Birmingham, 1974), Vol. IV, pp. 71 and 99–102.

[20]S. Ergun, J. Bayer, and W. V. Buren, J. Appl. Crystallogr. **38**, 3540 (1967).

[21]F. Utreras, Ph.D. thesis, University of Grenoble, 1979.

[22]T. E. Faber and J. M. Ziman, Philos. Mag. **11**, 153 (1965).

[23]K. Samwer and W. L. Johnson, Phys. Rev. B **28**, 2907 (1983).

[24]H. H. Paalman and C. J. Pings, J. Appl. Phys. **33**, 2635 (1962).

[25]J. R. D. Copley, in *Physics of Modern Materials*, edited by the IAEA (IAEA, Vienna, 1980), Vol. II, p. 613.

[26]J. A. Blech and B. L. Averbach, Phys. Rev. A **137**, 1113 (1965).

[27]J. L. Yarnell, M. J. Katz, R. G. Wenzel, and S. H. Koenig, Phys. Rev. A **7**, 2130 (1973).

[28]M. Maret, A. Pasturel, and P. Chieux, J. Phys. F **17**, 2191 (1987).

[29]Ph. Goudeau, A. Fontaine, A. Naudon, and C. E. Williams, J. Appl. Crystallogr. **19**, 19 (1986).

[30]Ph. Goudeau, A. Naudon, A. Chamberod, B. Rodmacq, and C. E. Williams, Laboratoire Pour l'Utilisation du Rayonne-Electromagnétique, Activity Report 1985–1987 (unpublished), p. 353.

[31]J. D. Gunton, M. San Miguel, and P. S. Sahni, in *Phase Transitions and Critical Phenomena*, edited by C. Domb and J. L. Lebowitz (Academic, London, 1983), p. 269.

[32]C. N. J. Wagner and H. Ruppersberg, At. Energy Rev. **1**, 101 (1981).

[33]A. J. Dianoux, B. Rodmacq, and A. Chamberod, J. Less-Common Met. **131**, 145 (1987). J. R. Beyster, Nucl. Sci. Eng. **31**, 254 (1968).

[34]J. H. Harris, W. A. Curtin, and M. A. Tenhover, Phys. Rev. B **36**, 5784 (1987).

[35]J. R. Beyster, Nucl. Sci. Eng. **31**, 254 (1968).

[36]P. Chieux, R. de Kouchkovsky, and B. Boucher, J. Phys. F **14**, 2239 (1984).